Synthesis and Reactions of Diphosphinidenecyclobutene Ruthenium Complexes Relevant to Catalytic Hydrosilylation of Terminal Alkynes

Akito Hayashi, Takahiko Yoshitomi, Kazutoshi Umeda, Masaaki Okazaki, and Fumiyuki Ozawa*

International Research Center for Elements Science (IRCELS), Institute for Chemical Research, Kyoto University, Uji, Kyoto 611-0011, Japan

Received February 9, 2008

The complex [RuCl(μ-Cl)(CO)(DPCB-OMe)]$_2$ (**1a**), bearing a low-coordinated phosphorus ligand (DPCB-OMe = 1,2-bis(4-methoxyphenyl)-3,4-bis[(2,4,6-tri-*tert*-butylphenyl)phosphinidene]cyclobutene), is readily reduced to [RuH(μ-Cl)(CO)(DPCB-OMe)]$_2$ (**2a**) by the reaction with water and $HSiMe_2Ph$. The reaction proceeds via a [$RuCl_2$(CO)(H_2O)(DPCB-OMe)] intermediate, which is characterized by X-ray diffraction analysis. Complexes **1a** and **2a** serve as highly efficient catalysts for *Z*-selective hydrosilylation of phenylacetylene. The reason for the high catalyst efficiency of DPCB-OMe complexes has been investigated by reaction and structure analysis of the presumed intermediate [Ru(CH=CHPh)Cl(CO)(DPCB-OMe)] (**3a**). It has been found that **3a** has ample space to associate with hydrosilane and, therefore, readily undergoes metathesis between Ru−C and H−Si bonds. This structural feature in conjunction with the strong π-accepting ability of the DPCB-OMe ligand leads to highly efficient catalysis for *Z*-selective hydrosilylation of terminal alkynes.

Introduction

Catalytic hydrosilylation of terminal alkynes is a simple and efficient way of synthesizing alkenylsilanes, which are widely used in organic synthesis.[1] While the reaction generally adopts a *syn*-addition process to afford (*E*)-alkenylsilanes, *anti*-addition giving (*Z*)-alkenylsilanes has also been documented using rhodium,[2] iridium,[3] and ruthenium catalysts.[4,5] As for ruthenium, Oro et al. reported a pioneering work showing highly *Z*-selective hydrosilylation of phenylacetylene catalyzed by [RuHCl(CO)($PiPr_3$)$_2$] (**2m**).[4a] This catalysis is applicable to several aromatic and aliphatic acetylenes,[4c,d] but a relatively large amount of **2m** is needed to gain high catalytic activity.[6] On the other hand, we recently found that [RuCl(μ-Cl)(CO)(DPCB-OMe)]$_2$ (**1a**), bearing a low-coordinated phosphorus ligand (DPCB-OMe),[7] exhibits much higher catalyst efficiency.[8] For example, reaction of PhC≡CH with $HSiMe_2Ph$ in CH_2Cl_2 in the presence of **1a** (0.25 mol %) is completed within 10 min at room temperature to afford (*Z*)-PhCH=CH$SiMe_2Ph$ in 98% selectivity,[8a] whereas the same reaction using **2m** (5 mol %) instead of **1a** takes 2 h for completion.[4c]

Scheme 1 shows the mechanism of catalytic hydrosilylation, which is illustrated on the basis of previous mechanistic observations using [RuHCl(CO)(PPh_3)$_3$] catalyst (**2n**).[9] The *Z*-selective catalytic cycle is presumed to involve silyl complex **4** as the key intermediate, although participation of polynuclear species derived from **4** cannot be excluded.[6] Thus, *trans*-insertion of alkyne into the Ru−Si bond of **4** (process (iv)),[10,11] followed by metathesis between the Ru−C bond of **5** and the Si−H bond of hydrosilane (process (v)),[9b] affords (*Z*)-alkenylsilane. Complex **4** may be isolated,[4c] but this catalytically active species is generally prepared in situ from **2** via alkenyl complex

* To whom correspondence should be addressed. E-mail: ozawa@scl.kyoto-u.ac.jp.

(1) (a) Ojima, I.; Li, Z.; Zhu, J. *The Chemistry of Organic Silicon Compounds*; Wiley: New York, 1998; p 1687. (b) Marciniec, B. *Comprehensive Handbook on Hydrosilylation*; Pergamon: Oxford, 1992; p 130. (c) Denmark, S. E.; Baird, J. D. *Chem.−Eur. J.* **2006**, *12*, 4954.

(2) (a) Takeuchi, R.; Tanouchi, N. *J. Chem. Soc., Perkin Trans. 1* **1994**, 2909. (b) Mori, A.; Takahisa, E.; Kajiro, H.; Hirabayashi, K.; Nishihara, Y.; Hiyama, T. *Chem. Lett.* **1998**, 443. (c) Mori, A.; Takahisa, E.; Kajiro, H.; Nishihara, Y.; Hiyama, T. *Macromolecules* **2000**, *33*, 1115. (d) Faller, J. W.; D'Alliessi, D. G. *Organometallics* **2002**, *21*, 1743. (e) Mori, A.; Takahisa, E.; Yamamura, Y.; Kato, T.; Mudalige, A. P.; Kajiro, H.; Hirabayashi, K.; Nishihara, Y.; Hiyama, T. *Organometallics* **2004**, *23*, 1755.

(3) (a) Tanke, R. S.; Crabtree, R. H. *J. Am. Chem. Soc.* **1990**, *112*, 7984. (b) Jun, C.-H.; Crabtree, R. H. *J. Organomet. Chem.* **1993**, *447*, 177. (c) Sridevi, V. S.; Fan, W. Y.; Leong, W. K. *Organometallics* **2007**, *26*, 1157.

(4) (a) Esteruelas, M. A.; Herrero, L. A.; Oro, L. A. *Organometallics* **1993**, *12*, 2377. (b) Na, Y.; Chang, S. *Org. Lett.* **2000**, *2*, 1887. (c) Katayama, H.; Taniguchi, K.; Kobayashi, M.; Sagawa, T.; Minami, T.; Ozawa, F. *J. Organomet. Chem.* **2002**, *645*, 192. (d) Katayama, H.; Nagao, M.; Moriguchi, R.; Ozawa, F. *J. Organomet. Chem.* **2003**, *676*, 49. (e) Aricó, C. S.; Cox, L. R. *Org. Biomol. Chem.* **2004**, *2*, 2558. (f) Maifeld, S. V.; Tran, M. N.; Lee, D. *Tetrahedron Lett.* **2005**, *46*, 105.

(5) Ruthenium catalysts giving 2-silyl-1-alkenes have also been reported: (a) Trost, B. M.; Ball, Z. T *J. Am. Chem. Soc.* **2001**, *123*, 12726. (b) Trost, B. M.; Ball, Z. T. *J. Am. Chem. Soc.* **2003**, *125*, 30. (c) Trost, B. M.; Ball, Z. T. *J. Am. Chem. Soc.* **2005**, *127*, 17644. (d) Kawanami, Y.; Sonoda, Y.; Mori, T.; Yamamoto, K. *Org. Lett.* **2002**, *4*, 2825. (e) Menozzi, C.; Dalko, P. I.; Cossy, J. *J. Org. Chem.* **2005**, *70*, 10717.

(6) Martin, M.; Sola, E.; Lahoz, F. J.; Oro, L. A. *Organometallics* **2002**, *21*, 4027.

(7) DPCB-OMe: 1,2-bis(4-methoxyphenyl)-3,4-bis[(2,4,6-tri-*tert*-butylphenyl)phosphinidene]cyclobutene. See for review: Ozawa, F.; Yoshifuji, M. *Dalton Trans.* **2006**, 4987.

(8) (a) Nagao, M.; Asano, K.; Umeda, K.; Katayama, H.; Ozawa, F. *J. Org. Chem.* **2005**, *70*, 10511. (b) Katayama, H.; Nagao, M.; Nishimura, T.; Matsui, Y.; Umeda, K.; Akamatsu, K.; Tsuruoka, T.; Nawafune, H.; Ozawa, F. *J. Am. Chem. Soc.* **2005**, *127*, 4350.

(9) (a) Maruyama, Y.; Yamamura, K.; Nakayama, I.; Yoshiuchi, K.; Ozawa, F. *J. Am. Chem. Soc.* **1998**, *120*, 1421. (b) Maruyama, Y.; Yamamura, K.; Sagawa, T.; Katayama, H.; Ozawa, F. *Organometallics* **2000**, *19*, 1308.

(10) Maddock, S. M.; Rickard, C. E. F.; Roper, W. R.; Wright, L. J. *Organometallics* **1996**, *15*, 1793.

(11) (a) For the mechanism of *trans*-insertion, see: (a) Ref 3a. (b) Ojima, I.; Clos, N.; Donovan, R. J.; Ingellina, P. *Organometallics* **1990**, *9*, 3127. (c) Chung, L. W.; Wu, Y.-D.; Trost, B. M.; Ball, Z. T. *J. Am. Chem. Soc.* **2003**, *125*, 11578.

10.1021/om800119f CCC: $40.75
Publication on Web 04/16/2008

Scheme 1

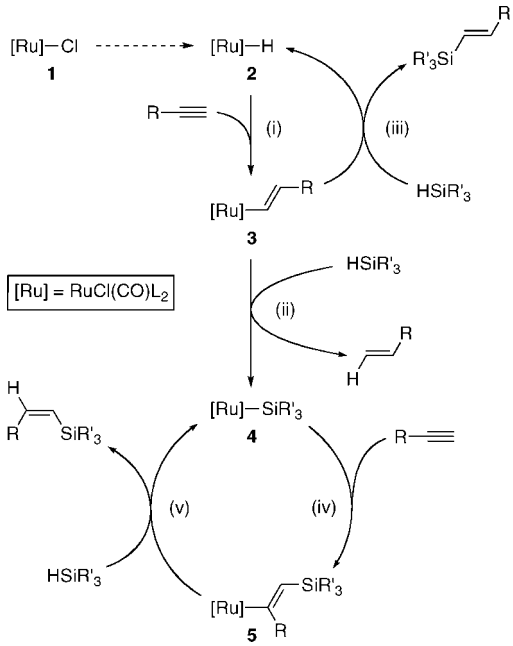

3 for a stability reason. Alkyne insertion into **2** (process (i)) proceeds spontaneously, whereas the subsequent reaction of **3** with hydrosilane (process (ii)) is a significantly slow process when catalyst **2m**, bearing bulky P*i*Pr$_3$ ligands, is employed as catalyst.[4a] Thus, the low catalyst efficiency of **2m** is mainly due to the poor reactivity of [Ru(CH═CHR)Cl(CO)(P*i*Pr$_3$)$_2$] (**3m**) toward hydrosilane.[12] The complex [Ru(CH═CHR)Cl(CO)(PPh$_3$)$_2$] (**3n**), bearing less bulky PPh$_3$ ligands, is sufficiently reactive, but predominantly undergoes C−Si bond formation process (iii) giving (*E*)-alkenylsilane.[9b]

This paper deals with the reason for the high catalyst efficiency of **1a**. On the basis of the mechanistic information described above, we set the following objectives: (i) the formation process of a hydrido complex (**2a**) from **1a**; (ii) the reactivity of **2a** toward PhC≡CH. It has been found that **1a** is cleanly converted to [RuH(μ-Cl)(CO)(DPCB-OMe)]$_2$ (**2a**) by the aid of water and HSiMe$_2$Ph.

Results and Discussion

Preparation of [RuCl(μ-Cl)(CO)(DPCB-OMe)]$_2$ (1a). The title compound was prepared referring to the synthetic procedure reported for the dppf analogue [RuCl(μ-Cl)(CO)(dppf)]$_2$ (eq 1).[13] A toluene solution of [Ru(η^3-allyl)Cl(CO)$_3$] and DPCB-OMe (1 equiv/Ru) was heated under reflux for 2 h. The resulting [Ru(η^3-allyl)Cl(CO)(DPCB-OMe)] was then reacted with an Et$_2$O solution of dry HCl (3 equiv/Ru) at room temperature, causing gradual precipitation of **1a** in 62% yield. Similarly, [RuCl(μ-Cl)(CO)(DPCB)]$_2$ and [RuCl(μ-Cl)(CO)(DPCB-CF$_3$)]$_2$ were prepared in 52 and 30% yields, respectively.[14]

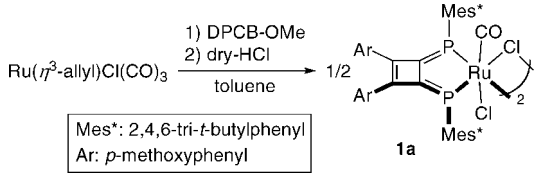

(1)

In the ^{1}H NMR spectrum of **1a**, the *tert*-butyl groups at the *ortho* positions of 2,4,6-tri-*tert*-butylphenyl substituents (Mes*) were observed as two singlet signals at δ 1.61 and 1.64. Since the Mes* groups are oriented orthogonal to the diphosphinidenecyclobutene skeleton and their rotation is sterically hindered,[15] the appearance of two signals may be taken as a strong indication of the presence of two different ligands at the apical positions of the Ru(DPCB-OMe) moiety. On the other hand, the ^{31}P{^{1}H} NMR spectrum exhibited only one singlet at δ 143.9, showing the coordination of the same ligands *trans* to the phosphorus atoms. Consequently, it is concluded that **1a** is a dinuclear complex symmetrically bridged by two μ-Cl ligands. The DPCB-OMe ligand adopts chelate coordination to the equatorial positions, whereas the CO and Cl ligands share the apical positions of each ruthenium center. Similar structures have been observed for related diphosphine complexes by X-ray analysis.[13,16] Unlike diphosphine analogues, which are flexible in solution and readily transformed into other geometrical isomers, **1a** was structurally stable in CD_2Cl_2 at room temperature.

Complex **1a** readily reacted with PPh$_3$ (1 equiv/Ru) in CH_2Cl_2 at room temperature to afford **6a** (eq 2) in 98% yield. The ^{31}P{^{1}H} NMR spectrum exhibited three sets of signals at δ 29.8 (dd, J_{PP} = 439 and 24 Hz), 125.3 (dd, J_{PP} = 24 and 12 Hz), and 136.6 (dd, J_{PP} = 439 and 12 Hz), which are assigned to PPh$_3$ (δ 29.8) and DPCB-OMe (δ 125.3 and 136.6), respectively. The signal pattern clearly indicates the *trans*,*cis*-disposition of PPh$_3$ against DPCB-OMe. Thus, the PPh$_3$ ligand is introduced to the equatorial position.

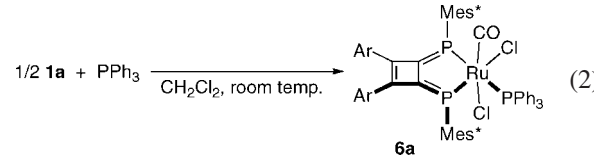

(2)

On the other hand, when **1a** was treated with carbon monoxide in CH_2Cl_2, a new carbonyl ligand was incorporated into the apical coordination site (eq 3). The reaction proceeded instantly at room temperature to give **7a**, exclusively. Since the complex could not be isolated, its structure was identified by IR and NMR spectroscopy. The ^{31}P{^{1}H} NMR spectrum showed a singlet at δ 123.6. The IR spectrum exhibited a weak ν(CO) band at 2112 cm^{-1} together with strong absorption at 2042 cm^{-1}, indicating a slightly bent arrangement of the CO ligands in mutually *trans* positions.

Complex **7a** gradually isomerized to thermodynamic product **7a′**, which was isolated as reddish-orange crystals in 81% yield. The ^{31}P{^{1}H} NMR spectrum exhibited two sets of signals at δ 128.5 and 136.5. The IR spectrum showed two ν(CO) bands at 2069 and 2005 cm^{-1}. These spectroscopic data are consistent with the *cis*,*cis*,*cis*-configuration around ruthenium.

Preparation of [RuH(μ-Cl)(CO)(DPCB-OMe)]$_2$ (2a). Complex **1a** was reduced by HSiMe$_2$Ph in CH_2Cl_2 at room temperature. Preliminary attempts using dry CH_2Cl_2 ([H$_2$O] <

(12) Complex **3m** is the only ruthenium species detected in the reaction solution using catalyst **2m**.[4a] On the other hand, the silyl complex [Ru(SiMe$_2$Ph)Cl(CO)(P*i*Pr$_3$)$_2$] (**4m**) prepared from [RuCl$_2$(CO)(P*i*Pr$_3$)$_2$] and LiSiMe$_2$Ph shows extremely high catalytic activity.[4c]

(13) Cadierno, V.; Crochet, P.; Díez, J.; García-Garrido, S. E.; Gimeno, J. *Organometallics* **2003**, *22*, 5226.

(14) DPCB: 1,2-diphenyl-3,4-bis[(2,4,6-tri-*tert*-butylphenyl)phosphinidene]cyclobutene. DPCB-CF$_3$: 1,2-bis(4-trifluoromethylphenyl)-3,4-bis[(2,4,6-tri-*tert*-butylphenyl)phosphinidene]cyclobutene.

(15) Ozawa, F.; Kawagishi, S.; Ishiyama, T.; Yoshifuji, M. *Organometallics* **2004**, *23*, 1325.

(16) (a) Drouin, S. D.; Amoroso, D.; Yap, G. P. A.; Fogg, D. E. *Organometallics* **2002**, *21*, 1042. (b) Samantha, D. D.; Sebastien, M.; Dino, A.; Yap, D. P. A.; Fogg, D. E. *Organometallics* **2005**, *24*, 4721. (c) Gottschalk-Gaudig, T.; Folting, K.; Caulton, K. G. *Inorg. Chem.* **1999**, *38*, 5241.

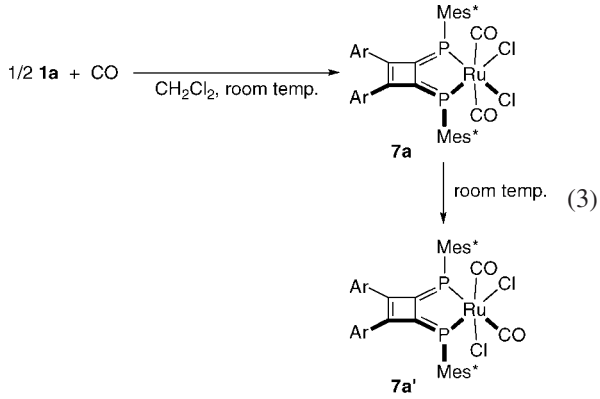

3 mM) occasionally formed a hydride species, but the reaction was not reproducible. Eventually, **1a** was cleanly converted to **2a** in the presence of a small amount of water, where the aqua complex **8a** serves as a key intermediate (Scheme 2).

Complex **1a** readily combined with residual water in CH_2Cl_2[17] to give an equilibrium mixture of **1a** and **8a** ($[\mathbf{8a}]^2/[\mathbf{1a}][H_2O] = 24$), from which red crystals of **8a** were precipitated. Figure 1 shows the X-ray structure. Two complex molecules in a unit cell (space group $P\bar{1}$, $Z = 2$) are associated with each other by O−H···Cl type hydrogen bonds (O2···Cl2′ = 3.193(6) Å). Each molecule adopts a slightly distorted octahedral configuration around ruthenium. The CO and H_2O ligands at the apical positions are tilted away from the bulky Mes* groups (C1−Ru−O2 = 171.9(2)°). The Ru−O2(aqua) distance is within the range of ruthenium aqua complexes (2.11–2.25 Å).[18]

Treatment of **8a** with $HSiMe_2Ph$ (100 equiv/Ru) in CD_2Cl_2 at room temperature led to selective formation of **2a**, along with $HOSiMe_2Ph$ and $PhMe_2SiOSiMe_2Ph$ as byproducts.[19] The use of excess $HSiMe_2Ph$ was essential to obtain **2a** cleanly; otherwise the reaction was a significantly slow process involving partial decomposition of ruthenium species. Accordingly, **2a** could not be isolated, but its formation was indicated by the appearance of a triplet signal assignable to RuH at δ –8.44 (J_{PH} = 12 Hz) in the ^1H NMR spectrum. Since the ^{31}P NMR signal (^1H nondecoupled) was observed as a doublet with the same J_{PH} coupling at δ 160.8, **2a** was assigned to a dinuclear complex bearing a hydride ligand at the apical position of each ruthenium center (Scheme 2). The complex readily reacted with PPh_3 to give **10a**, which was independently prepared from **6a** and fully characterized. The RuH signal of **10a** was observed at δ –9.81 (ddd, J_{PH} = 155, 30, and 18 Hz). The $^{31}P\{^1H\}$ NMR signals showed an ABX pattern that is consistent with meridional coordination of phosphorus atoms of DPCB-OMe and PPh_3 ligands.

Although the aqua complex **8a** was involved, the formation of **2a** was prevented by excess water (10 equiv/Ru). On the other hand, the reaction was effectively accelerated by DBU (1 equiv/Ru) and proceeded even at 0 °C with a relatively small amount of $HSiMe_2Ph$ (25 equiv/Ru). Thus, it is reasonable that the aqua complex **8a** is in equilibrium with the hydroxy complex **9a**, which reacts with $HSiMe_2Ph$ via a four-membered transition state (**A**) to afford **2a** and silanol. Actually, when **8a** was treated with DBU (1 equiv/Ru) in the absence of $HSiMe_2Ph$, the $^{31}P\{^1H\}$ NMR signal of **8a** at δ 134.4 instantly decreased, and a new singlet assignable to **9a** appeared at δ 145.2 (**8a**/**9a** = 45/55).

Reaction of 2a with Phenylacetylene and $HSiMe_2Ph$. Complex **2a** generated in situ from **8a** and $HSiMe_2Ph$ (100 equiv/Ru) in CH_2Cl_2 was treated with excess phenylacetylene (105 equiv/Ru) at 0 °C. GLC analysis revealed the formation of styrene and (*Z*)- and (*E*)-styrylsilanes together with a small amount of $PhC{\equiv}CSiMe_2Ph$ (1%). As seen from the time-course in Figure 2, styrene (4%, 5 equiv/Ru) and (*E*)-styrylsilane (6%) are formed only at the initial stage, whereas the amount of (*Z*)-styrylsilane continuously increases until the end of the reaction.[20]

Scheme 3 reasonably accounts for the product distribution in Figure 2. Similarly to the monophosphine systems in Scheme 1, the DPCB-OMe complex **2a** readily undergoes insertion of phenylacetylene (process (i)). As indirect evidence, it was observed that the RuH signal of **2a** instantly disappears upon treatment with phenylacetylene (1 equiv/Ru) at −30 °C. The styryl complex **3a** subsequently reacts with $HSiMe_2Ph$ via two reaction processes, (ii) and (iii), giving styrene and (*E*)-styrylsilane, respectively. Process (ii) irreversibly converts **3a** to **4a**, whereas process (iii) reproduces **2a** and then **3a**. As a result, all ruthenium species are shifted to **4a**, and thereafter the (*Z*)-styrylsilane formation via processes (iv) and (v) is exclusively operative. In this case, a stoichiometric amount of styrene should be formed, while a catalytic amount of styrene (5 equiv/Ru) was generated in reality. This is probably due to the presence of a side reaction converting **4a** to **2a** with the aid of water or $HOSiMe_2Ph$ (process (vi)). Actually, the formation of a comparable amount of $PhMe_2SiOSiMe_2Ph$ (5 equiv/Ru) was observed in the reaction system.[21]

The Reason for High Catalyst Efficiency of the DPCB-OMe Complex. It has been found that DPCB-OMe styryl complex **3a** generated from **2a** and phenylacetylene reacts smoothly with $HSiMe_2Ph$ even at 0 °C. The observed reactivity is clearly higher than that of monophosphine analogues.[6,9] Since it was previously observed that the reactivity of [Ru(alkenyl)Cl(CO)$(PPh_3)_2$] complexes toward hydrosilane is strongly affected by steric conditions around ruthenium,[9b] the structure of **3a** was examined by DFT calculations using a model compound (**3a′**) having 2,6-dimethylphenyl groups instead of 2,4,6-tri-*tert*-butylphenyl groups (Mes*).

Figure 3 shows the optimized structures of **3a′** and related dppe complex **3b**, together with the X-ray structure of [Ru(CH=CHC_6H_4OMe-*p*)Cl(CO)$(PPh_3)_2$] (**3n′**).[9b] Complexes **3a′** and **3b** have very similar structures to each other. Both complexes adopt a square-pyramidal configuration around ruthenium having one of the phosphorus atoms at the apical

(17) Commercial grade CH_2Cl_2 containing ca. 25 mM of water as confirmed by the Karl−Fischer analysis.

(18) (a) Stanko, J. A.; Chaipayungpundhu, S. *J. Am. Chem. Soc.* **1970**, *92*, 5580. (b) Boniface, S. M.; Clark, G. R.; Collins, T. J.; Roper, W. R. *J. Organomet. Chem.* **1981**, *206*, 109. (c) Harding, P. A.; Preece, M.; Robinson, S. D. *Inorg. Chim. Acta* **1986**, *118*, L31. (d) Bergmeister, J. J., III; Hanson, B. E. ; Merola, J. S. *Inorg. Chem.* **1990**, *29*, 4831. (e) Kölle, U.; Flunkert, G.; Görissen, R.; Schmidt, M. U.; Englert, U. *Angew. Chem., Int. Ed.* **1992**, *31*, 440. (f) Sun, Y.; Taylor, N. J.; Carty, A. J. *Inorg. Chem.* **1993**, *32*, 4457. (g) Mahon, M. F.; Whittlesey, M. K.; Wood, P. T. *Organometallics* **1999**, *18*, 4068. (h) Goicoechea, J. M.; Mahon, M. F.; Whittlesey, M. K.; Anil Kumar, P. G.; Pregosin, P. S. *Dalton Trans.* **2005**, 588.

(19) Siloxane ($PhMe_2SiOSiMe_2Ph$ may be formed by dehydrative dimerization of silanol ($HOSiMe_2Ph$) catalyzed by HCl, which is generated from **8a** in the formation of **9a**.

(20) The *Z*-selectivity of styrylsilane reaches 94% at the end of the reaction; the value is somewhat lower than that observed at room temperature (98%).[8a]

(21) It has been confirmed that the amounts of styrene and $PhMe_2SiOSiMe_2Ph$ are nearly twice the amount of residual water in the system, showing the following stoichiometry:

$$2\,PhC{\equiv}CH + H_2O + 2\,HSiMe_2Ph \xrightarrow{\textbf{2a (catalyst)}} 2\,PhCH{=}CH_2 + 2\,PhMe_2SiOSiMe_2Ph$$

Scheme 2. Reaction Processes for Conversion of 1a to 2a

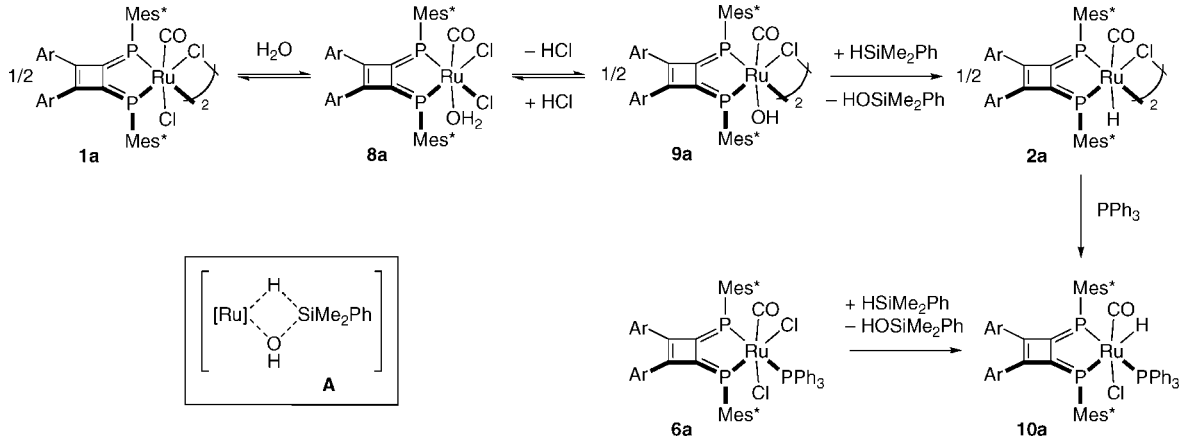

position. The styryl ligand is situated *trans* to the other phosphorus atom; the P−Ru−C angles are 175.5° (**3a′**) and 171.9° (**3b**), respectively. As a result, the front side of the RuCH=CHPh moiety is widely opened. In contrast, complex **3n′** is apparently more crowded and the ruthenium center is sterically protected by PPh_3 ligands. Accordingly, it is reasonable that **3a** associates easily with hydrosilane to cause C−H and C−Si bond formation processes (ii) and (iii). This structural feature is very probably due to the chelate coordination of the DPCB-OMe ligand with a small bite angle (ca. 83°). Since the dppe complex **3b** has similar steric conditions around ruthenium, we next examined the catalytic activity of $[RuCl(\mu\text{-}Cl)(CO)(dppe)]_2$ (**1b**) toward hydrosilylation of terminal alkynes.

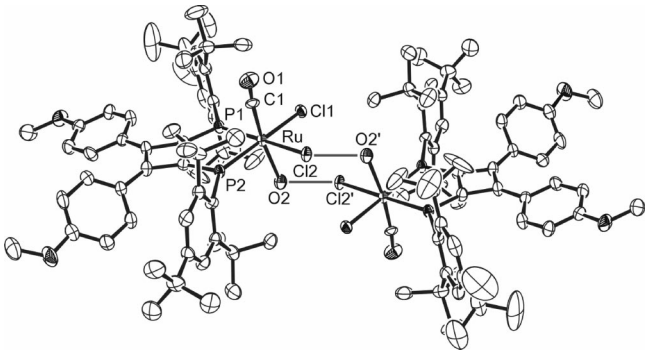

Figure 1. ORTEP drawing of **8a**·CH_2Cl_2 with thermal ellipsoids at the 50% probability level. All hydrogen atoms and the molecule of CH_2Cl_2 are omitted for clarity. Selected bond distances (Å) and angles (deg): Ru−P1 = 2.356(3), Ru−P2 = 2.348(4), Ru−Cl1 = 2.391(4), Ru−Cl2 = 2.440(3), Ru−O2 = 2.194(6), Ru−C1 = 1.832(7), C1−O1 = 1.129(8), P1−Ru−P2 = 83.01(12), Cl1−Ru−Cl2 = 90.41(12), C1−Ru−O2 = 171.9(2), Ru−C1−O1 = 174.2(6).

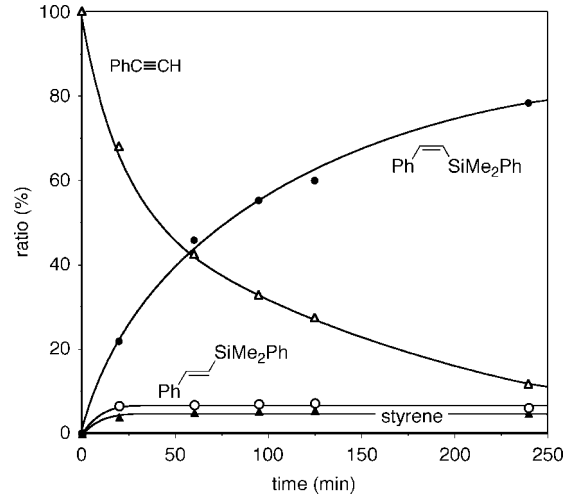

Figure 2. Time-course of the reaction of phenylacetylene (0.52 mmol) with $HSiMe_2Ph$ (0.49 mmol) catalyzed by **2a** (4.9 μmol). The reaction was conducted in CH_2Cl_2 (0.5 mL) at 0 °C and followed by GLC using toluene as an internal standard.

Table 1 lists the results. The dppe complex **1b** is somewhat less reactive than **1a**, but much more efficient than **2m**, bearing $PiPr_3$ ligands (runs 1–3). As for the product selectivity, **1b** is inferior to **1a**, especially for the reactions of *para*-substituted phenylacetylenes and 1-octyne (runs 4–11).

As seen from Scheme 1, the ratio of (*Z*)- and (*E*)-alkenylsilanes is controlled by the relative ease of processes (ii) and (iii). Process (iii) affords (*E*)-alkenylsilane via C−Si bond formation, whereas process (ii) leads to C−H bond formation giving silyl complex **4** as the carrier of the *Z*-selective catalytic cycle. These processes must involve an alkenyl complex coordinated with hydrosilane (**11**) as the common intermediate (Scheme 4). It is likely that DPCB-OMe, as a strong π-acceptor ligand,[15] effectively stabilizes the electron-rich silyl complex **4** to facilitate process (ii) leading to *Z*-selective hydrosilylation.

Conclusion

We have observed that complex **1a** is cleanly reduced by water and hydrosilane, where aqua complex **8a** and hydroxy complex **9a** serve as key intermediates (Scheme 2). A similar process has been reported for iridium systems.[22] The resulting hydride **2a** catalyzes conversion of phenylacetylene into (*E*)- and (*Z*)-styrylsilanes and styrene. The formation of (*E*)-styrylsilane and styrene is finished at the initial stage, and thereafter (*Z*)-styrylsilane is selectively formed (Figure 2). Scheme 3 rationalizes this phenomenon. First, complex **2a** undergoes insertion of phenylacetylene to give styryl complex **3a**, which subsequently reacts with hydrosilane via two reaction processes, (ii) and (iii). These processes are competitively operative with each other. However, since process (iii) reproduces **3a** whereas process (ii) exclusively converts **3a** to silyl complex **4a**, all catalytic species are ultimately shifted to the *Z*-selective catalytic cycle. DFT calculations have suggested that **3a** has ample space to associate with hydrosilane (Figure 3). This structural feature is remarkable as compared with monophosphine complexes and should be responsible for the high catalyst efficiency of **1a**.

(22) Luo, X.-L.; Crabtree, R. H. *J. Am. Chem. Soc.* **1989**, *111*, 2527.

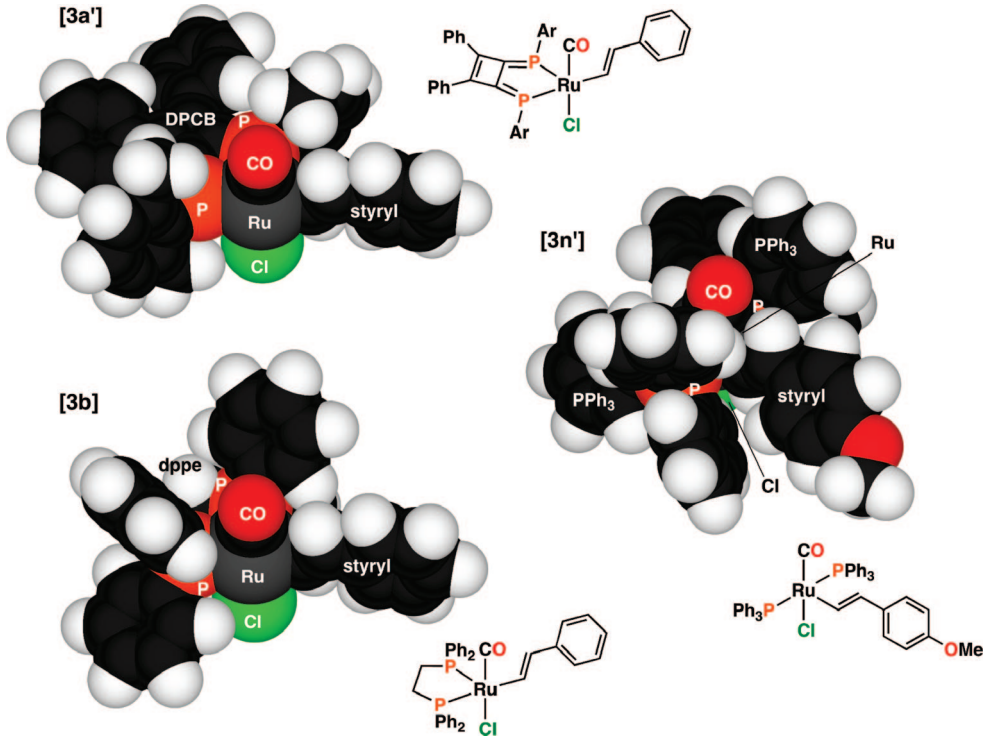

Figure 3. Comparison of calculated (**3a′**, **3b**) and X-ray structures (**3n′**) of styryl complexes.

Scheme 3. Hydrosilylation Mechanism of Phenylacetylene Catalyzed by 2a

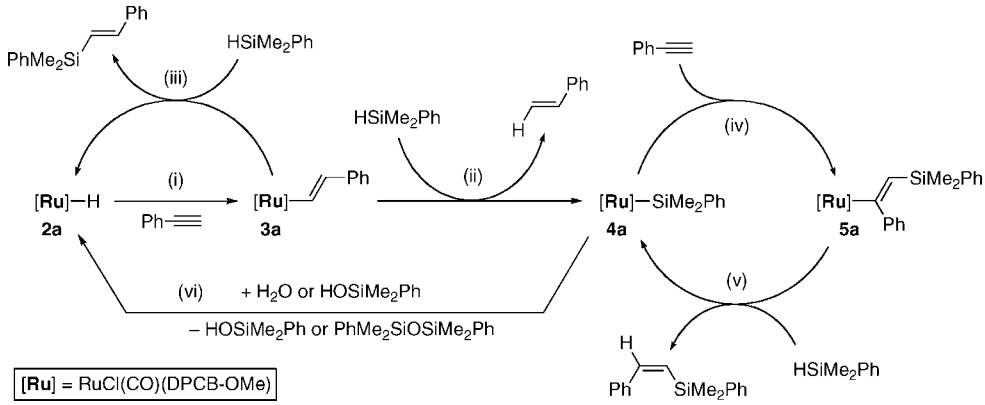

Table 1. Catalytic Hydrosilylation of RC≡CH with $HSiMe_2Ph$[a]

run	alkyne (R)	catalyst[b] (mol %)	solvent	time	conversion[c] (%)	product ratio[d] [*Z*/*E*/*gem*]
1	Ph	**1a** (0.25)	CH_2Cl_2	10 min	100	98/1/1
2	Ph	**1b** (0.25)	CH_2Cl_2	40 min	100	96/4/0
3	Ph	**2m** (5)	CH_2Cl_2	2 h	100	97/3/0
4	4-$MeOC_6H_4$	**1a** (1)	toluene	2 h	100	99/1/0
5	4-$MeOC_6H_4$	**1b** (1)	toluene	2 h	100	49/51/0
6	4-$CF_3C_6H_4$	**1a** (0.5)	toluene	5 h	100	97/1/2
7	4-$CF_3C_6H_4$	**1b** (0.5)	toluene	5 h	48	72/28/0
8	4-$MeO_2C_6H_4$	**1a** (0.25)	CH_2Cl_2	3 h	100	97/1/2
9	4-$MeO_2C_6H_4$	**1b** (0.25)	CH_2Cl_2	5 h	66	62/32/6
10	*n*-C_6H_{13}	**1a** (1)	toluene	5 h	100	97/1/2
11	*n*-C_6H_{13}	**1b** (1)	toluene	5 h	8	36/64/0

[a] Reactions were run with RC≡CH (1.05 mmol), $HSiMe_2Ph$ (1 mmol), and solvent (1 mL) at room temperature. [b] **1a**: [$RuCl(\mu\text{-}Cl)(CO)(DPCB\text{-}OMe)]_2$; **1b**: [$RuCl(\mu\text{-}Cl)(CO)(dppe)]_2$; **2m**: [$RuHCl(CO)(P{i}Pr_3)_2$]. [c] Determined by GLC. [d] Determined by ^1H NMR spectroscopy. *gem*-isomer: $CH_2{=}CR(SiMe_2Ph)$.

Scheme 4

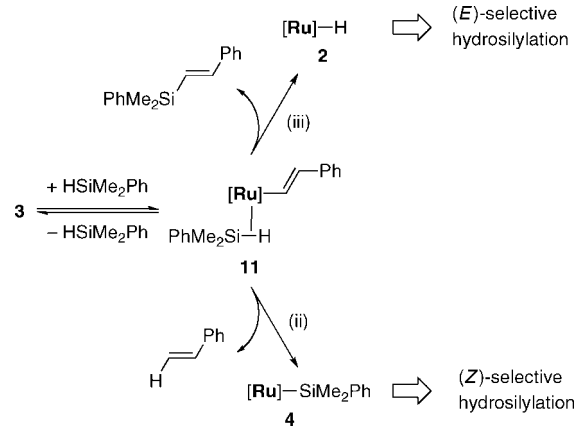

Experimental Section

General Considerations. All manipulations were performed under a nitrogen atmosphere using conventional Schlenk techniques unless otherwise noted. NMR spectra were recorded on a Varian Mercury 300 spectrometer (^1H NMR 300 MHz, ^{13}C NMR 75.5 MHz, ^{31}P NMR 121.5 MHz). IR spectra were recorded on a JASCO FT/IR-410 instrument. Elemental analysis was performed by the ICR Analytical Laboratory, Kyoto University. The compounds

$[Ru(\eta\text{-}C_3H_5)Cl(CO)_3]$[23] and DPCB-Y (Y = OMe, H, CF_3)[15] were synthesized according to the literature.

Preparation of $[RuCl(\mu\text{-}Cl)(CO)(DPCB\text{-}OMe)]_2$ (1a). A solution of $[Ru\eta^3\text{-}C_3H_5)Cl(CO)_3]$ (154 mg, 0.590 mmol) and DPCB-OMe (484 mg, 0.594 mmol) in toluene (5.9 mL) was refluxed for 2 h with stirring. The dark red solution was cooled to room temperature, and a solution of dry HCl in Et_2O (1.1 M, 1.61 mL, 1.77 mmol) was added. The mixture was stirred at room temperature overnight to give a red precipitate of **1a**, which was collected by filtration, washed with Et_2O (3 mL × 2) at −30 °C, and dried under vacuum (370 mg, 62%). The complexes $[RuCl(\mu\text{-}Cl)(CO)(dppe)]_2$ (**1b**), $[RuCl(\mu\text{-}Cl)(CO)(DPCB)]_2$ (**1c**), and $[RuCl(\mu\text{-}Cl)(CO)(DPCB\text{-}CF_3)]_2$ (**1d**) were similarly prepared in 49, 52, and 30% yields, respectively. The complexes were identified by NMR and IR spectroscopy and elemental analysis, while the $^{13}C\{^1H\}$ NMR spectra were not observed for solubility reasons.

1a. Mp: 246 °C. IR (KBr): 1995 cm^{-1} (s). ^1H NMR (CD_2Cl_2, 20 °C): δ 1.36 (s, 36H, *p*-^{t}Bu), 1.61 (s, 36H, *o*-^{t}Bu), 1.64 (s, 36H, *o*-^{t}Bu), 3.68 (s, 12H, OMe), 6.37 (d, J_{HH} = 9.2 Hz, 8H, Ar), 6.43 (d, J_{HH} = 9.2 Hz, 8H, Ar), 7.40 (s, 4H, *m*-PAr), 7.44 (s, 4H, *m*-PAr). $^{31}P\{^1H\}$ NMR (CD_2Cl_2, 20 °C): δ 143.9 (s). Anal. Calcd for $C_{110}H_{144}Cl_4O_6P_4Ru_2$: C, 65.08; H, 7.15. Found: C, 64.98; H, 7.10.

1b. Mp: 250 °C. IR (KBr): 1977 cm^{-1} (s). ^1H NMR (CD_2Cl_2, 20 °C): δ 2.63 (m, 4H, CH_2), 3.00 (m, 4H, CH_2), 7.41 (m, 24H, Ph), 7.78 (m, 8H, Ph), 7.94 (m, 8H, Ph). $^{31}P\{^1H\}$ NMR (CD_2Cl_2, 20 °C): δ 65.5 (s). Anal. Calcd for $C_{54}H_{48}Cl_4O_2P_4Ru_2$: C, 54.19; H, 4.04. Found: C, 53.93; H, 4.17.

1c. Mp: 235 °C. IR (KBr): 1994 cm^{-1} (s). ^1H NMR (CD_2Cl_2, 20 °C): δ 1.34 (s, 36H, *p*-^{t}Bu), 1.62 (s, 36H, *o*-^{t}Bu), 1.64 (s, 36H, *o*-^{t}Bu), 6.51 (d, J_{HH} = 7.6 Hz, 8H, *o*-Ar), 6.87 (t, J_{HH} = 7.8 Hz, 8H, *m*-Ar), 7.08 (t, J_{HH} = 7.4 Hz, 4H, *p*-Ar), 7.38 (s, 4H, *m*-PAr), 7.41 (s, 4H, *m*-PAr). $^{31}P\{^1H\}$ NMR (CD_2Cl_2, 20 °C): δ 153.3 (s). Anal. Calcd for $C_{106}H_{136}Cl_4O_2P_4Ru_2$: C, 66.65; H, 7.18. Found: C, 66.50; H, 7.07.

1d. Mp: 235 °C. IR (KBr): 2009 cm^{-1} (s). ^1H NMR (CD_2Cl_2, 20 °C): δ 1.34 (s, 36H, *p*-^{t}Bu), 1.62 (s, 36H, *o*-^{t}Bu), 1.64 (s, 36H, *o*-^{t}Bu), 6.61 (d, J_{HH} = 8.4 Hz, 8H, *o*-Ar), 7.14 (d, J_{HH} = 8.4 Hz, 8H, *m*-Ar), 7.43 (s, 8H, *m*-PAr). $^{31}P\{^1H\}$ NMR (CD_2Cl_2, 20 °C): δ 164.9 (s). Anal. Calcd for $C_{110}H_{134}Cl_4F_{12}O_2P_4Ru_2$: C, 60.49; H, 6.18. Found: C, 60.30; H, 6.00.

Preparation of $[RuCl_2(CO)(PPh_3)(DPCB\text{-}OMe)]$ (6a). A solution of **1a** (101 mg, 0.0497 mmol) and PPh_3 (26.1 mg, 0.100 mmol) in CH_2Cl_2 (3.2 mL) was stirred for 5 min at room temperature. Volatile materials were removed under reduced pressure. The residue was dissolved in a minimum amount of CH_2Cl_2, layered with pentane, and allowed to stand at room temperature to give orange crystals of **6a** (124 mg, 98%). Mp: 175 °C. IR (KBr): 1964 cm^{-1} (s). ^1H NMR (CD_2Cl_2, 20 °C): δ 1.27 (s, 9H, *o*-^{t}Bu), 1.41 (s, 9H, *o*-^{t}Bu), 1.46 (s, 9H, *p*-^{t}Bu), 1.48 (s, 9H, *p*-^{t}Bu), 1.63 (s, 9H, *o*-^{t}Bu), 1.70 (s, 9H, *o*-^{t}Bu), 3.67 (s, 3H, OMe), 3.71 (s, 3H, OMe), 6.34 (d, 2H, J_{HH} = 8.7 Hz, Ar), 6.42 (d, 2H, J_{HH} = 8.7 Hz, Ar), 6.49 (d, 2H, J_{HH} = 8.7 Hz, Ar), 6.60 (d, 2H, J_{HH} = 8.7 Hz, Ar), 7.10 (t, 6H, J_{HH} = 6.6 Hz, Ph), 7.31 (t, 3H, J_{HH} = 6.6 Hz, Ph), 7.53–7.66 (m, 10H, *m*-PAr and Ph). $^{13}C\{^1H\}$ NMR (CD_2Cl_2, 20 °C): δ 31.5, 31.6, 34.2, 34.3, 34.7, 35.0, 35.6, 35.7, 39.0 (d, J_{PC} = 2 Hz), 39.2 (d, J_{PC} = 2 Hz), 39.9 (d, J_{PC} = 2 Hz), 39.9 (d, J_{PC} = 2 Hz), 55.5 (OMe), 55.5 (OMe), 113.7, 113.7, 114.0, 114.1, 123.2 (d, J_{PC} = 8 Hz), 123.3 (d, J_{PC} = 8 Hz), 124.5 (d, J_{PC} = 8 Hz), 125.9 (d, J_{PC} = 8 Hz), 126.5, 127.3, 127.3, 127.6 (d, J_{PC} = 10 Hz), 129.8 (d, J_{PC} = 2 Hz), 129.9 (d, J_{PC} = 2 Hz), 130.2 (d, J_{PC} = 3 Hz), 130.3 (d, J_{PC} = 2 Hz), 130.4 (d, J_{PC} = 2 Hz), 132.9 (d, J_{PC} = 3 Hz), 133.5 (d, J_{PC} = 3 Hz), 135.6 (d, J_{PC} = 9 Hz), 153.4 (m, P═C*C*), 154.9, 157.6 (d, J_{PC} = 2 Hz), 157.8, 159.3, 160.7 (d, J_{PC} = 3 Hz), 160.7 (d, J_{PC} = 3 Hz), 177.6 (m, P═C), 198.9 (m, CO). $^{31}P\{^1H\}$ NMR (CD_2Cl_2, 20 °C): δ 29.8 (dd, J_{PP} = 439 and 24 Hz), 125.3 (dd, J_{PP} = 24 and 12 Hz), 136.6 (dd, J_{PP} = 439 and 12 Hz). Anal. Calcd for $C_{73}H_{87}Cl_2O_3P_3Ru$: C, 68.64; H, 6.86. Found: C, 68.59; H, 7.10.

Preparation of $[RuCl_2(CO)_2(DPCB\text{-}OMe)]$ (7a and 7a′). The CO gas was passed through a suspension of **1a** (200 mg, 0.0985 mmol) in CH_2Cl_2 (5.0 mL) at room temperature. The mixture quickly changed to a red homogeneous solution. The $^{31}P\{^1H\}$ NMR spectrum showed the selective formation of **7a**. IR (CH_2Cl_2): 2112 (w), 2042 cm^{-1} (s). ^1H NMR (CD_2Cl_2, 20 °C): δ 1.43 (s, 18H, *p*-^{t}Bu), 1.65 (s, 36H, *o*-^{t}Bu), 3.70 (s, 6H, OMe), 6.42 (br, 8H, Ar), 7.56 (m, 4H, *m*-PAr). $^{31}P\{^1H\}$ NMR (CD_2Cl_2, 20 °C): δ 123.6 (s).

The solution of **7a** thus prepared was stirred for 7 h at room temperature. Volatile substances were removed under reduced pressure. The residue was dissolved in a minimum amount of CH_2Cl_2, layered with Et_2O, and allowed to stand at room temperature to give orange crystals of **7a′** (167 mg, 81%). Mp: 224 °C. IR (KBr): 2069 (s), 2005 cm^{-1} (s). ^1H NMR ($CDCl_3$, 20 °C): δ 1.41 (s, 18H, *p*-^{t}Bu), 1.63 (s, 18H, *o*-^{t}Bu), 1.66 (s, 18H, *o*-^{t}Bu), 3.71 (s, 3H, OMe), 3.72 (s, 3H, OMe), 6.38–6.48 (m, 8H, Ar), 7.48–7.54 (m, 4H, *m*-PAr). $^{13}C\{^1H\}$ NMR ($CDCl_3$, 20 °C): δ 31.4, 31.5, 33.9, 34.0, 34.3, 34.3, 35.5, 38.5 (d, J_{PC} = 2 Hz), 38.9 (d, J_{PC} = 2 Hz), 38.9 (d, J_{PC} = 2 Hz), 39.3 (d, J_{PC} = 2 Hz), 55.2 (OMe), 113.8, 113.8, 121.9 (d, J_{PC} = 9 Hz), 122.4 (d, J_{PC} = 9 Hz), 122.6 (d, J_{PC} = 9 Hz), 122.9 (d, J_{PC} = 9 Hz), 123.4, 123.5, 124.9, 125.1, 129.1 (d, J_{PC} = 1 Hz), 129.2 (d, J_{PC} = 1 Hz), 129.4 (d, J_{PC} = 1 Hz), 129.5 (d, J_{PC} = 1 Hz), 153.8 (m, *P* = C*C*), 157.2, 157.6, 159.4 (d, *J* = 3 Hz), 159.7 (d, *J* = 2 Hz), 160.5 (d, *J* = 4 Hz), 160.6 (d, *J* = 4 Hz), 175.8 (dd, J_{PC} = 57 and 19 Hz, P═C), 176.9 (dd, J_{PC} = 41 and 16 Hz, P═C), 189.7 (dd, J_{PC} = 147 and 12 Hz, CO), 192.4 (dd, J_{PC} = 17 and 13 Hz, CO). $^{31}P\{^1H\}$ NMR ($CDCl_3$, 20 °C): δ 128.5 (s), 136.5 (s). Anal. Calcd for $C_{60}H_{82}Cl_2O_5P_2Ru$: C, 64.50; H, 7.40. Found: C, 64.32; H, 7.01.

Preparation of $[RuCl_2(CO)(H_2O)(DPCB\text{-}OMe)]$ (8a). Complex **1a** (15.0 mg, 7.38 μmol) was dissolved in CH_2Cl_2 (1.0 mL) containing a small amount of water (ca. 25 mM)[17] and allowed to stand at room temperature. Red crystals of **8a** were precipitated over hours. The product was collected by filtration, washed with Et_2O, and dried under vacuum (15.0 mg, 98%). Mp: 255 °C. IR (KBr): 1989 cm^{-1} (s). ^1H NMR (CD_2Cl_2, 20 °C): δ 1.46 (s, 18H, *p*-^{t}Bu), 1.61 (s, 18H, *o*-^{t}Bu), 1.68 (s, 18H, *o*-^{t}Bu), 2.73 (br, 2H, H_2O), 3.73 (s, 6H, OMe), 6.45 (d, J_{HH} = 7.2 Hz, 4H, Ar), 6.51 (d, J_{HH} = 8.4 Hz, 4H, Ar), 7.59 (s, 2H, *m*-PAr), 7.61 (s, 2H, *m*-PAr). $^{31}P\{^1H\}$ NMR (CD_2Cl_2, 20 °C): δ 134.4 (s). Anal. Calcd for $C_{55}H_{74}Cl_2O_4P_2Ru$: C, 63.94; H, 7.22. Found: C, 64.23; H, 7.05.

Preparation of $[Ru(OH)(\mu\text{-}Cl)(CO)(DPCB\text{-}OMe)]_2$ (9a) (NMR Tube Reaction). Complex **1a** (5.0 mg, 2.46 μmol) was dissolved in CD_2Cl_2 (0.5 mL) containing a small amount of water (ca. 25 mM), and a solution of 1,8-diazabicyclo[5.4.0]undec-7-ene (DBU) in CD_2Cl_2 (48.9 mM, 101 μL, 4.93 μmol, 1 equiv/Ru) was added at 0 °C. The color of the solution instantly changed from red to deep red. The $^{31}P\{^1H\}$ NMR spectrum showed the formation of a new species assignable to **9a** in addition to **8a** (**8a**/**9a** = 45/55). ^1H NMR (CD_2Cl_2, 20 °C): δ 1.41 (s, 36H, *p*-^{t}Bu), 1.64 (br, 72H, *o*-^{t}Bu), 3.68 (s, 12H, OMe), 6.37–6.42 (m, 16H, Ar), 7.47 (s, 4H, *m*-PAr), 7.50 (s, 4H, *m*-PAr). $^{31}P\{^1H\}$ NMR (CD_2Cl_2, 20 °C): δ 145.2 (s).

Preparation of $[RuH(Cl)(CO)(DPCB\text{-}OMe)]_2$ (2a) (NMR Tube Reaction). Complex **1a** (5.0 mg, 2.46 μmol) was dissolved in CD_2Cl_2 (0.5 mL) containing a small amount of water (ca. 25 mM). $HSiMe_2Ph$ (67.2 mg, 0.493 mmol, 100 equiv/Ru) was added at 0 °C, and the mixture was allowed to stand at room temperature for 1 h. The NMR spectra showed the selective formation of **2a**. ^1H NMR (CD_2Cl_2, −5 °C): δ −8.44 (t, J_{PH} = 12 Hz, 1H, Ru*H*). ^{31}P NMR (CD_2Cl_2, −5 °C): δ 160.8 (d, J_{PH} = 12 Hz).

The same reaction was examined in the presence of DBU. A solution of **2a** was prepared from **1a** (5.0 mg, 2.46 μmol) and

(23) Sbrana, B.; Braca, G.; Piacenti, F.; Pino, P. *J. Organomet. Chem.* **1968**, *13*, 240.

Table 2. Crystallographic Data for 8a·CH_2Cl_2

formula	$C_{56}H_{76}Cl_4O_4P_2Ru$
fw	1117.98
cryst size, mm	0.10 × 0.06 × 0.05
cryst syst	triclinic
a (Å)	14.556(15)
b (Å)	14.86(2)
c (Å)	15.45(2)
α (deg)	81.08(11)
β (deg)	64.64(9)
γ (deg)	71.75(10)
V (Å^3)	2869(6)
space group	$P\bar{1}$ (#2)
Z	2
d_{calcd} (g cm^{-3})	1.294
μ (Mo Kα) (mm^{-1})	0.557
θ range (deg)	3.15–27.48
no. of reflns collected	22 289
no. of unique reflns	12 235 (R_{int} = 0.0593)
transmn factor	0.9464–0.9727
no. of reflns with I > 2*σ*(*I*)	8335
no. of variables	624
goodness-of-fit on F^2	1.119
final *R* indices (*I* > 2*σ*(*I*))	R1 = 0.0797, wR2 = 0.2292
R indices (all data)	R1 = 0.1178, wR2 = 0.3074

CD_2Cl_2 (0.5 mL) containing a small amount of water (ca. 25 mM) at room temperature. $HSiMe_2Ph$ (0.123 mmol, 25 equiv/Ru) and DBU (4.93 *μ*mol, 1 equiv/Ru) were successively added, and the sample solution was allowed to stand at room temperature. The $^{31}P\{^1H\}$ NMR spectrum showed exclusive formation of **2a** (*δ* 160.8).

Preparation of [RuH(Cl)(CO)(PPh_3)(DPCB-OMe)] (10a). To a solution of **6a** (62.0 mg, 0.0485 mmol) in CH_2Cl_2 (2.5 mL) was added $HSiMe_2Ph$ (13.2 mg, 0.0970 mmol). The solution was stirred at 40 °C for 1.5 h. Volatile materials were removed under reduced pressure. The residue was washed with pentane and recrystallized from Et_2O/pentane to give **10a** as an orange powder (46.0 mg, 78%). Mp: 145 °C. IR (KBr): 1938 cm^{-1} (CO). ^1H NMR (CD_2Cl_2, 20 °C): *δ* −9.81 (ddd, J_{PH} = 155, 30 and 18 Hz, 1H, Ru*H*), 1.19 (s, 9H, *o*-^{t}Bu), 1.40 (s, 9H, *p*-^{t}Bu), 1.45 (s, 9H, *p*-^{t}Bu), 1.52 (s, 9H, *o*-^{t}Bu), 1.55 (s, 9H, *o*-^{t}Bu), 1.78 (s, 9H, *o*-^{t}Bu), 3.67 (s, 3H, OMe), 3.70 (s, 3H, OMe), 6.34 (d, J_{HH} = 9.2 Hz, 2H, Ar), 6.42 (d, J_{HH} = 8.8 Hz, 2H, Ar), 6.56 (d, J_{HH} = 8.0 Hz, 2H, Ar), 6.58 (d, J_{HH} = 7.2 Hz, 2H, Ar), 7.14–7.18 (m, 6H, Ph), 7.27–7.31 (m, 3H, Ph), 7.37 (s, 2H, *m*-PAr), 7.49 (s, 2H, *m*-PAr), 7.61–7.66 (m, 6H, Ph). $^{13}C\{^1H\}$ NMR (CD_2Cl_2, 20 °C): *δ* 31.8, 31.8, 34.7, 34.7, 35.7, 39.1, 39.5, 39.6, 39.7, 55.6 (OMe), 55.7 (OMe), 113.8, 114.1, 123.0 (d, J_{PC} = 5 Hz), 123.3 (d, J_{PC} = 5 Hz), 124.2 (d, J_{PC} = 5 Hz), 124.7 (d, J_{PC} = 5 Hz), 127.9 (d, J_{PC} = 10 Hz), 129.7 (d, J_{PC} = 5 Hz), 129.8, 130.3 (d, J_{PC} = 5 Hz), 135.4 (d, J_{PC} = 10 Hz), 135.9, 136.3, 152.7 (m, P═C*C*), 155.3, 157.7, 157.8, 158.8, 160.3 (d, J_{PC} = 3 Hz), 160.4 (d, J_{PC} = 3 Hz), 176.9–177.7 (m, P═C), 201.9–202.3 (m, CO). $^{31}P\{^1H\}$ NMR (CD_2Cl_2, 20 °C): *δ* 48.8 (dd, J_{PP} = 362 and 15 Hz), 148.2 (dd, J_{PP} = 362 and 19 Hz), 150.0 (dd, J_{PP} = 19 and 15 Hz). Anal. Calcd for $C_{77}H_{98}ClO_4P_3Ru$: C, 70.22; H, 7.50. Found: C, 70.05; H, 7.69.

Reaction of 2a with Phenylacetylene and $HSiMe_2Ph$. A solution of **2a** (4.92 *μ*mol) was prepared from **1a** (5.0 mg, 2.46 *μ*mol), $HSiMe_2Ph$ (67.2 mg, 0.493 mmol), and wet CH_2Cl_2 (0.5 mL). Phenylacetylene (52.8 mg, 0.517 mmol) was added at 0 °C, and the amounts of organic compounds in the system were analyzed at intervals by GLC using toluene as an internal standard.

DFT Calculations. The geometry optimization of compounds **3a′** and **3b** was carried out with the program package Gaussian 98[24] using B3LYP in conjunction with the SDD basis set and effective core potential for Ru and 6-31G(d) basis set for other atoms.

X-ray Structural Analysis of 8a. The X-ray diffraction study was performed on a Rigaku Mercury CCD diffractometer with graphite-monochromated Mo Kα radiation (*γ* = 0.71070 Å). The intensity data were collected at 173 K and corrected for Lorentz and polarization effects and absorption (numerical). The structure was solved by DIRDIF99[25] and refined by full-matrix least-squares procedures on F^2 for all reflections (SHELXL-97).[26] Hydrogen atoms except for those of the H_2O ligand were placed using AFIX instructions. Crystallographic data have been deposited with the Cambridge Crystallographic Center: CCDC No. 671813. A summary of the data is given in Table 2.

Acknowledgment. This work was supported by Grants-in-Aid for Scientific Research on Priority Areas (No. 18064010, "Synergy of Elements") from the Ministry of Education, Culture, Sports, Science, and Technology, Japan.

Supporting Information Available: Tables with Cartesian coordinates of the optimized structures of **3a′** and **3b**; crystallographic data of **8a** in cif format. This material is available free of charge via the Internet at http://pubs.acs.org.

OM800119F

(24) Frisch, M. J.; Trucks, G. W.; Schlegel, H. B.; Scuseria, G. E.; Robb, M. A.; Cheeseman, J. R.; Zakrzewski, V. G.; Montgomery Jr., J. A.; Stratmann, R. E. ; Burant, J. C. ; Dapprich, S.; Millam, J. M.; Daniels, A. D.; Kudin, K. N.; Strain, M. C.; Farkas, O.; Tomasi, J.; Barone, V.; Cossi, M.; Cammi, R.; Mennucci, B.; Pomelli, C.; Adamo, C.; Clifford, S.; Ochterski, J.; Petersson, G. A.; Ayala, P. Y.; Cui, Q.; Morokuma, K.; Malick, D. K.; Rabuck, A. D.; Raghavachari, K.; Foresman, J. B.; Cioslowski, J.; Ortiz, J. V.; Stefanov, B. B.; Liu, G.; Liashenko, A.; Piskorz, P.; Komaromi, I.; Gomperts, R.; Martin, R. L.; Fox, D. J.; Keith, T.; Al-Laham, M. A.; Peng, C. Y.; Nanayakkara, A.; Gonzalez, C.; Challacombe, M.; Gill, P. M. W.; Johnson, B.; Chen, W.; Wong, M. W.; Andres, J. L.; Gonzalez, C.; Head-Gordon, M.; Replogle, E. S.; Pople, J. A. *Gaussian 98, Revision A.9*; Gaussian, Inc.: Pittsburgh, PA, 1998.

(25) Beurskens, P. T.; Beurskens, G.; de Gelder, R.; García-Grana, S.; Gould, R. O.; Israel, R.; Smits, J. M. M. *The DIRDIF99 Program System*; University of Nijmegen: The Netherlands, 1999.

(26) Sheldrick, G. M. *SHELXL-97*; University of Göttingen: Germany, 1997.